



## Sensitive Test for Ion-Cyclotron Resonant Heating in the Solar Wind

Justin C. Kasper,<sup>1,\*</sup> Bennett A. Maruca,<sup>2</sup> Michael L. Stevens,<sup>1</sup> and Arnaud Zaslavsky<sup>3</sup>

<sup>1</sup>Harvard-Smithsonian Center for Astrophysics, Cambridge, Massachusetts 02138, USA

<sup>2</sup>Space Sciences Laboratory, University of California, Berkeley, California 94720, USA

<sup>3</sup>LESIA, Observatoire de Paris, CNRS, UPMC, Université Paris Diderot, 92190 Meudon, France

(Received 2 November 2012; published 28 February 2013)

Plasma carrying a spectrum of counterpropagating field-aligned ion-cyclotron waves can strongly and preferentially heat ions through a stochastic Fermi mechanism. Such a process has been proposed to explain the extreme temperatures, temperature anisotropies, and speeds of ions in the solar corona and solar wind. We quantify how differential flow between ion species results in a Doppler shift in the wave spectrum that can prevent this strong heating. Two critical values of differential flow are derived for strong heating of the core and tail of a given ion distribution function. Our comparison of these predictions to observations from the Wind spacecraft reveals excellent agreement. Solar wind helium that meets the condition for strong core heating is nearly 7 times hotter than hydrogen on average. Ion-cyclotron resonance contributes to heating in the solar wind, and there is a close link between heating, differential flow, and temperature anisotropy.

DOI: [10.1103/PhysRevLett.110.091102](https://doi.org/10.1103/PhysRevLett.110.091102)

PACS numbers: 96.60.P-, 52.30.Ex, 52.35.Mw

*Introduction.*—The solar corona and solar wind are so tenuous that wave-particle interactions can dominate over fluid or collisional processes, resulting in highly nonthermal plasma as seen by spacecraft in interplanetary space. Heavier ions escape from the Sun at higher speeds than the ionized hydrogen ( $H^+$ ) that dominates the solar wind. Within a given solar wind stream, different species flow through one another at speeds of up to several hundred  $\text{km s}^{-1}$  [1,2]. This differential flow appears to be stable as long as it is aligned with the local magnetic field  $\mathbf{B}$  and below the Alfvén wave speed  $C_A$  [3,4]. Heavier ions are also often much hotter than  $H^+$ , with temperatures reaching and often exceeding mass proportionality [5–8]. These nonthermal properties can be used to identify the role wave-particle interactions play in heating the corona and solar wind [9–11]. If we can understand the underlying physics, we will be able to predict the relative heating of ions and electrons in the solar wind, the corona, and other magnetized plasmas.

Candidate theories that can produce both the observed temperature profiles and nonthermal ion signatures generally build on the dissipation of a given type of fluctuation or small-scale structure in the plasma [12–16]. In these models, different types of waves couple directly to a subset of ions or electrons in phase space resulting in preferential heating of certain species and the observed nonthermal ion properties. Examples include oblique kinetic Alfvén waves [17], fast magnetosonic waves [18], current sheets [19], and magnetic reconnection exhausts [20]. In this Letter, we focus on stochastic heating due to resonant interactions between ions and ion-cyclotron waves [15,21,22]. In this theory, all ions can resonate with a single ion-cyclotron wave and be weakly heated, but certain ions with mass/charge greater than  $H^+$  can interact with counterpropagating waves and experience

stronger heating as a result of a second-order Fermi process. Our motivation for this focus is threefold. First, there may be a sufficient level of power in Alfvénic fluctuations in the solar wind to sustain this mode of heating [23,24]. Second, ion-cyclotron resonance could explain the large temperature anisotropies [2,8,25] and growing magnetic moments seen with distance from the Sun [26]. Finally, we propose that of the theories listed, only the ion-cyclotron mechanism is consistent with the precise relations between ion heating and plasma conditions reported herein.

Denote the dimensionless Alfvén Mach number of the field-aligned differential flow of species  $i$  relative to  $H^+$  by  $\delta v_{ip} \equiv (\mathbf{V}_i - \mathbf{V}_p) \cdot \mathbf{B} / (|\mathbf{B}|C_A)$ , where  $\mathbf{V}_p$  and  $\mathbf{V}_i$  denote vector velocities of the  $H^+$  and species  $i$ , respectively (for  $\text{He}^{2+}$ ,  $i = \alpha$ ). The key to this work is that finite  $\delta v_{ip}$  can prevent a species from experiencing the second-order Fermi process. Numerical simulations have shown that the efficiency of heavy ion heating decreases for nonzero  $\delta v_{ip}$  [27–29]. This dependence has also been investigated in the solar wind by comparing the properties of the  $H^+$  and  $\text{He}^{2+}$  that account for the bulk of the solar wind [28,30,31]. Those studies found that  $\text{He}^{2+}$  is hotter and more anisotropic than  $H^+$  when  $|\delta v_{\alpha p}| \lesssim 0.2$ , and that  $H^+$  is more anisotropic than  $\text{He}^{2+}$  when  $|\delta v_{\alpha p}| \neq 0$  [28,31]. We now use the theory of ion-cyclotron resonant heating to develop quantitative predictions for the dependence of heating on  $\delta v_{ip}$ .

*Theory.*—The velocity distribution function (VDF) of the thermal core of each species of ion in the solar wind is generally observed to fit a bi-Maxwellian distribution, with separate temperatures  $T_{\perp i}$  and  $T_{\parallel i}$  perpendicular and parallel to  $\mathbf{B}$ , respectively [32]. In the  $H^+$  frame each species moves along  $\mathbf{B}$  with mean speed  $\delta v_{ip}C_A$  and thermal width of  $w_{\parallel i}$ , where  $k_B T_{\parallel i} = 1/2 m_i w_{\parallel i}^2$ . We will

assume that the rate at which an ion species is preferentially heated is proportional to the fraction of the VDF that can simultaneously resonate with counterpropagating ion-cyclotron waves.

Efficient energy exchange is possible whenever an ion with gyrofrequency  $\Omega_i = q_i B/m_i$  encounters an ion-cyclotron wave with the same frequency. Resonant ions are transported through velocity space on an arc about the phase speed of the wave. Any one wave-particle interaction with random phase is equally likely to raise or lower the energy of a single ion, but net heating of the entire population is possible if there is a favorable gradient in the density of the VDF along the resonant path in velocity space. To identify the possible wave-particles resonances, we use the cold plasma dispersion relation for parallel propagating ion cyclotron waves,

$$\frac{\omega(k)}{\Omega_p} = \frac{|k|C_A}{\Omega_p} \sqrt{1 - \omega/\Omega_p}, \quad (1)$$

where  $\omega$  is the frequency and  $k$  is the wave number. Under Eq. (1) waves move with phase speed  $\leq C_A$ , meaning that especially for plasma with  $C_A > w_{\parallel i}$  there is an opportunity for significant heating.

A single ion moving along  $\mathbf{B}$  with speed  $v_{\parallel i}$  relative to  $\mathbf{V}_p$  can resonantly scatter if the Doppler-shifted frequency  $\omega' = \omega(k) - kv_{\parallel i}$  of the ion-cyclotron wave equals the gyrofrequency of the ion,

$$\omega(\vec{k}) - kv_{\parallel i} = \Omega_i. \quad (2)$$

Normalizing Eq. (2) by  $\Omega_p$  and defining  $\delta v_{\parallel i} = v_{\parallel i}/C_A$ , we can also write the resonance condition as

$$\frac{\omega(k)}{\Omega_p} = \frac{|k|C_A}{\Omega_p} \delta v_{\parallel i} + \frac{\Omega_i}{\Omega_p}. \quad (3)$$

This allows us to plot the resonance criterion and dispersion relation on the same axes in Fig. 1 for individual  $\text{H}^+$  and  $\text{He}^{2+}$  ions flowing at several different  $\delta v_{\parallel i}$ . Each resonance line has slope  $v_{\parallel i}/C_A$  and intercepts the y axis at  $\Omega_i/\Omega_p$ , as indicated for several common species. The gold circles along each resonance line indicate which ion-cyclotron waves each ion can resonate with. Regardless of  $v_{\parallel p}$ , each  $\text{H}^+$  ion can only interact with ion-cyclotron waves at a single  $k$  and  $\omega$ . This single wave interaction results in limited perpendicular heating wherein the  $\text{H}^+$  diffuse through velocity space along arcs, and the resulting distinctive VDF shape has been observed in the solar wind [33].

Now consider the resonance lines for  $\text{He}^{2+}$  in Fig. 1.  $\text{He}^{2+}$  ions, or indeed any other species with  $\Omega_i < \Omega_p$ , can simultaneously interact with counterpropagating waves as long as their  $\delta v_{\parallel i}$  is below some species-dependent value. Simultaneous resonance frees these ions from the circumscribed arcs of the singly resonant  $\text{H}^+$ , permitting a more general diffusion through velocity space [15,21,22]. It is

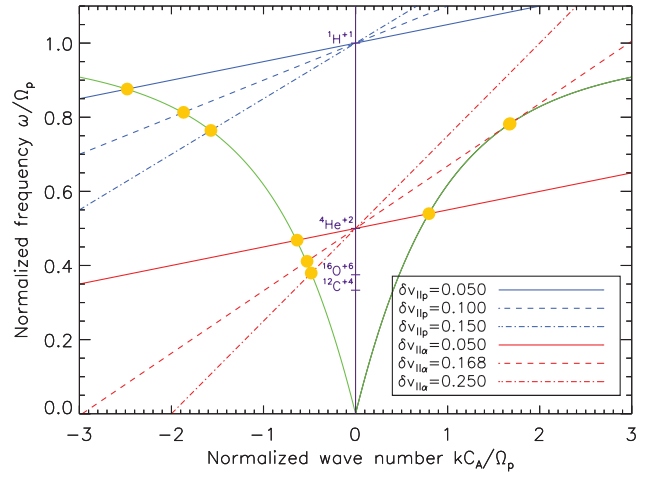


FIG. 1 (color). The dispersion relation for parallel propagating ion-cyclotron waves (green curve) and the resonance criteria given in Eq. (2) for  $\text{H}^+$  (top, blue) and  $\text{He}^{2+}$  (bottom, red) streaming along  $\mathbf{B}$  at different  $\delta v_{\parallel i}$ . Gold circles indicate wave resonances.

this general diffusion that permits ions other than  $\text{H}^+$  to experience significant and preferential heating perpendicular to  $\mathbf{B}$ .

As  $\delta v_{\parallel \alpha}$  increases, the slopes of the resonance line increase until Doppler shift prevents the  $\text{He}^{2+}$  from interacting with half of the spectrum of waves. There is a critical speed  $v_{oi}$  for each species at which Eq. (3) is tangent to Eq. (1), and beyond which ions cannot experience multiple resonance and instead behave like  $\text{H}^+$ . Solving for  $v_{oi}$ , we obtain

$$v_{oi} = \frac{2\{1 + \Omega_i/(2\Omega_p) - [2\Omega_i/\Omega_p + \Omega_i^2/(2\Omega_p)^2]^{1/2}\}^{3/2}}{2 + \Omega_i/(2\Omega_p) - [2\Omega_i/\Omega_p + \Omega_i^2/(2\Omega_p)^2]^{1/2}}, \quad (4)$$

which is a function only of  $\Omega_i/\Omega_p$ , or equivalently  $q_i/m_i$ . For  $\text{He}^{2+}$ ,  $v_{o\alpha} \approx 0.168$ , and  $v_{oi}$  increases monotonically with decreasing  $\Omega_i/\Omega_p$ .

Now consider the entire VDF of some species. For a given combination of  $\delta v_{ip}$  and  $w_{\parallel i}$ , some fraction of the VDF will extend below  $v_{oi}$ , and those particles will resonate with counterpropagating waves. We propose two key threshold values of  $\delta v_{ip}$ . The first,

$$\delta v_{ip}^c \equiv v_{oi}, \quad (5)$$

is the threshold for significant heating of the core of an ion species. When  $|\delta v_{ip}| < \delta v_{ip}^c$ , more than half of the ions can experience multiple resonance. As  $|\delta v_{ip}|$  rises above  $\delta v_{ip}^c$ , less of the population can come into resonance. When the  $|\delta v_{ip}| = v_{oi} + w_{\parallel i}/C_A$ , only particles in the tail of the distribution, more than one thermal width from the core, are able to experience multiple resonance. We define our second threshold, beyond which only the tail of an ion distribution can be heated strongly, accordingly as

$$v_{ip}^t \equiv \delta v_{ip}^c + w_{\parallel i}/C_A \approx v_{oi} + \beta_{\parallel p}^{1/2}, \quad (6)$$

where we have used  $\beta_{\parallel p} \equiv n_p k_B T_{\parallel p}/(B^2/2\mu_0) \approx w_{\parallel p}^2/C_A^2$  and  $w_{\parallel i} \approx w_{\parallel p}$  to simplify (6) and relate it to the ratio of thermal proton and magnetic pressure.

Improvements to this analysis could include substituting Eq. (1) with a more realistic dispersion relation and considering different scaling relationships between ion thermal speeds.

*Observations.*—We now look for evidence of these thresholds for core and tail heating of  $H^+$  and  $He^{2+}$  in the solar wind. We examined  $T_{\perp\alpha}/T_{\perp p}$ , the ratio of their temperatures perpendicular to  $\mathbf{B}$ , and  $T_{\perp p}/T_{\parallel p}$ , the  $H^+$  temperature anisotropy, as a function of  $\beta_{\parallel p}$  and  $\delta v_{\alpha p}$ . Based on our theory, we expect to observe the following three distinct zones in the  $\beta_{\parallel p} - \delta v_{\alpha p}$  plane.

(1) Independently of  $\beta_{\parallel p}$ , when  $|\delta v_{\alpha p}| < \delta v_{\alpha p}^c$ , the  $He^{2+}$  will be superheated perpendicular to  $\mathbf{B}$ , with a temperature significantly exceeding mass proportionality ( $T_{\perp\alpha}/T_{\perp p} > 4$ ).

(2) For  $\delta v_{\alpha p}^c < |\delta v_{\alpha p}| < \delta v_{\alpha p}^t$ , a diminishing, but still significant, fraction of the  $He^{2+}$  will experience strong heating;  $T_{\perp\alpha}/T_{\perp p}$  will drop, but still be above 4.

(3) Finally, when  $|\delta v_{\alpha p}| > \delta v_{\alpha p}^c$ , strong heating is restricted to the high energy tail of the  $He^{2+}$  VDF. By virtue of the fact that  $H^+$  far outnumbers  $He^{2+}$  [34], the  $H^+$  will absorb the majority of the wave power in this regime.  $T_{\perp\alpha}/T_{\perp p}$  will be lower still in this regime, while  $T_{\perp p}/T_{\parallel p}$  will be elevated as the  $H^+$  ions experience cyclotron resonant heating.

We use several million merged individual ion and magnetic field measurements from the Wind spacecraft from late 1994 through 2011 [32]. We followed previously documented procedures to select the subset of measurements for this study [34]. That work also examined solar wind conditions as a function of the Coulomb collision frequencies. In this Letter, we focus only on the approximately 30% of the solar wind with low collision frequencies.

Figure 2 shows the mean value of  $T_{\perp\alpha}/T_{\perp p}$  in the  $\beta_{\parallel p} - \delta v_{\alpha p}$  plane. Note that since  $V_{\alpha} \geq V_p$ , changes in the sign of  $\delta v_{\alpha p}$  just indicate the polarity of  $\mathbf{B}$ . The algorithm used to generate Figs. 2 and 3 is identical. The  $\beta_{\parallel p} - \delta v_{\alpha p}$  plane is divided into an initial grid with coarse resolution in  $\beta_{\parallel p}$  and  $\delta v_{\alpha p}$ . Each element in the grid is then subdivided as long as the resulting quadrants each have at least 100 observations. This process is iterated recursively, resulting in a plot with uniform uncertainty in the mean, and higher resolution in  $\delta v_{\alpha p}$  and  $\beta_{\parallel p}$  when their occurrence rate in the solar wind permits. The two dashed horizontal lines indicate  $\delta v_{\alpha p}^c \approx \pm 0.168$ , the critical flows below which the core of the  $He^{2+}$  VDF can resonate with counterpropagating waves. The solid lines indicate  $\pm \delta v_{ip}^t$ . For  $\beta_{\parallel p} \leq 2$ , there is a clear association between  $\delta v_{\alpha p}^c$  and

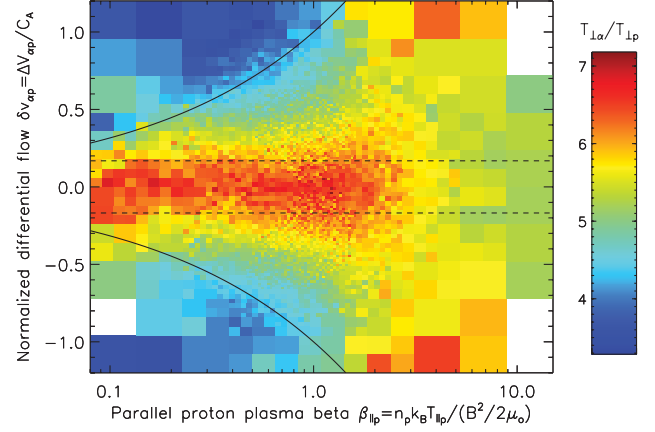


FIG. 2 (color).  $T_{\perp\alpha}/T_{\perp p}$  in the  $\beta_{\parallel p} - \delta v_{\alpha p}$  plane. Dashed lines indicate  $\pm \delta v_{\alpha p}^c$ , the speed below which the core of the  $He^{2+}$  VDF should experience multiple resonance. Solid lines indicate  $\delta v_{ip}^t$ , the speed beyond which only the tail of the  $He^{2+}$  is heated.

hot  $He^{2+}$ , with a mean  $T_{\perp\alpha}/T_{\perp p} \approx 7$ . As  $|\delta v_{\alpha p}|$  rises above  $\delta v_{\alpha p}^c$ ,  $T_{\perp\alpha}/T_{\perp p}$  begins to drop, as expected. When  $|\delta v_{\alpha p}|$  exceeds  $\delta v_{\alpha p}^t$ , and only a diminishing portion of the tail of the  $He^{2+}$  distribution can experience strong heating,  $T_{\perp\alpha}/T_{\perp p}$  drops below 4. This is all consistent with the first and second predictions of the theory enumerated above, although the drop in  $T_{\perp\alpha}/T_{\perp p}$  for  $\beta_{\parallel p} > 2$  remains unexplained.

Next we consider Fig. 3, which shows the  $H^+$  temperature anisotropy factor  $T_{\perp p}/T_{\parallel p}$  as a function of  $\delta v_{\alpha p}$  and  $\beta_{\parallel p}$ . On average, in the solar wind at 1 AU,  $T_{\perp p}/T_{\parallel p} \approx 0.8$ , and it is generally less than unity [25]. Figure 3 confirms that  $T_{\perp p}/T_{\parallel p} < 1$  over most of the parameter space. The anisotropy factor is significantly greater than unity,

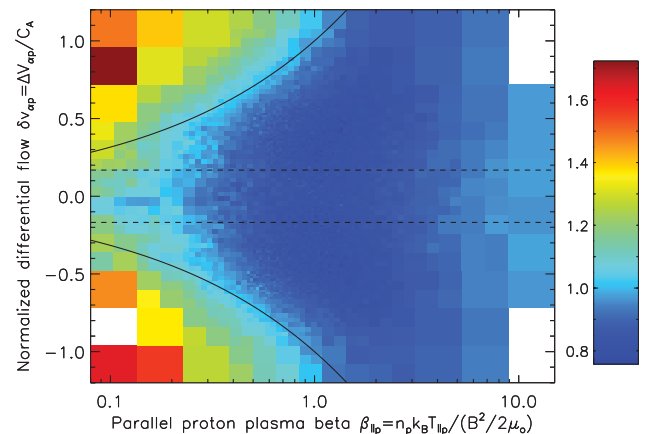


FIG. 3 (color).  $H^+$  temperature anisotropy  $T_{\perp p}/T_{\parallel p}$  in the  $\beta_{\parallel p} - \delta v_{\alpha p}$  plane. Threshold conditions are the same as in Fig. 2. When  $|\delta v_{\alpha p}| > \delta v_{ip}^t$  and the  $He^{2+}$  become nonresonant, the  $H^+$  take on a large anisotropy consistent with cyclotron resonance.

however, when  $|\delta v_{\alpha p}| > \delta v_{\alpha p}^t$ . This result is consistent with prediction (3) above.

*Conclusions.*—We have shown that the collisionless solar wind at 1 AU bears strong evidence of enhanced  $\text{He}^{2+}$  heating when the differential flow between  $\text{He}^{2+}$  and  $\text{H}^+$  is small compared to the Alfvén speed. The signature of this heating clearly delineates three regimes in the  $\beta_{\parallel p} - \delta v_{\alpha p}$  plane of strong, partial, and negligible relative heating, respectively. In this Letter, we used a specific wave-heating theory to produce an analytic prescription for the three regimes: in the strong heating regime, at least half of the  $\text{He}^{2+}$  VDF is cyclotron resonant with both ingoing and outgoing Alfvén waves simultaneously; in the partial heating regime, a portion of the core is resonant with both; and in the negligible heating regime, only the tail of the VDF is resonant with both.

The regimes predicted by the theory firmly agree with those observed in nature. The two critical differential flow speeds separating the three regimes have been derived in the theory and also demonstrated by spacecraft observations. The first,  $\delta v_{ip}^c$ , which separates the strong and partial heating regimes, is a function only of the ion cyclotron frequency ratio,  $\Omega_i/\Omega_p$ . For the alpha-proton case observed here, the threshold occurs at  $\delta v_{\alpha p} \approx 0.168$ . The second threshold,  $\delta v_{ip}^t$ , beyond which only the high speed tail of the ion velocity distribution experiences strong heating, is a function of  $\Omega_i/\Omega_p$  and  $\beta_{\parallel p}$ . Our results affirm that sufficient counterpropagating ion-cyclotron waves are available at  $0.5 \leq kC_A/\Omega_p \leq 3$  to heat ions through a stochastic Fermi mechanism.

While the solar wind data are consistent with this theory, several interesting features remain unexplained. Why, for example, does the occurrence of hot  $\text{He}^{2+}$  for  $|\delta v_{\alpha p}| < \delta v_{\alpha p}^c$  vanish for  $\beta_{\parallel p} > 2$ ? One likely hypothesis is that, for  $\beta_{\parallel p} \geq 1$ , Landau damping and transit-time damping of kinetic Alfvén waves is the dominant dissipation mechanism [17]. It could also be that the cold plasma approximation is insufficient for high  $\beta_{\parallel p}$ . Further insight could be gained by incorporating more realistic dispersion relations and by examining other ions.

Where exactly has this heating occurred? The amount of power in parallel propagating waves at 1 AU is a matter of debate [16]. Some models suggest counterpropagating waves are much more intense in the sub-Alfvénic corona, below 10–15 solar radii [35]. Our observations, however, show a very sharp dependence on  $\delta v_{\alpha p}^c$  as calculated with the *local* value of  $C_A$ . Because  $C_A$  decreases by an order of magnitude between the low corona and 1 AU, this implies either that the heating has occurred in interplanetary space or that some process maintains  $\delta v_{ip}$  near its coronal value. These controversies will be resolved by the upcoming NASA Solar Probe Plus mission, which will approach to within 9.5 solar radii of the center of the Sun and sample the sub-Alfvénic corona directly.

This work was supported by NASA Grant No. NNX12AB19G. The authors gratefully acknowledge productive discussions with S. Bale, B. Chandran, S. Cranmer, S. P. Gary, P. Isenberg, and W. Matthaeus.

\*jkasper@cfa.harvard.edu

- [1] M. Neugebauer, *J. Geophys. Res.* **81**, 78 (1976).
- [2] E. Marsch, K.-H. Mühlhäuser, H. Rosenbauer, R. Schwenn, and F.M. Neubauer, *J. Geophys. Res.* **87**, 35 (1982).
- [3] D. B. Reisenfeld, S. P. Gary, J. T. Gosling, J. T. Steinberg, D. J. McComas, B. E. Goldstein, and M. Neugebauer, *J. Geophys. Res.* **106**, 5693 (2001).
- [4] L. Berger, R. F. Wimmer-Schweingruber, and G. Gloeckler, *Phys. Rev. Lett.* **106**, 151103 (2011).
- [5] P. Bochsler, J. Geis, and R. Joos, *J. Geophys. Res.* **90**, 10779 (1985).
- [6] R. Hernandez, S. Livi, and E. Marsch, *J. Geophys. Res.* **92**, 7723 (1987).
- [7] R. von Steiger, J. Geiss, G. Gloeckler, and A. B. Galvin, *Space Sci. Rev.* **72**, 71 (1995).
- [8] S. R. Cranmer, G. B. Field, and J. L. Kohl, *Astrophys. J.* **518**, 937 (1999).
- [9] S. R. Cranmer, W. H. Matthaeus, B. A. Breech, and J. C. Kasper, *Astrophys. J.* **702**, 1604 (2009).
- [10] B. A. Maruca, J. C. Kasper, and S. D. Bale, *Phys. Rev. Lett.* **107**, 201101 (2011).
- [11] P. Hellinger, L. Matteini, Š. Štverák, P. M. Trávníček, and E. Marsch, *J. Geophys. Res.* **116**, A09105 (2011).
- [12] P. A. Isenberg and J. V. Hollweg, *J. Geophys. Res.* **88**, 3923 (1983).
- [13] C.-Y. Tu and E. Marsch, *J. Geophys. Res.* **106**, 8233 (2001).
- [14] S. R. Cranmer and A. A. van Ballegoijen, *Astrophys. J.* **594**, 573 (2003).
- [15] P. A. Isenberg and B. J. Vasquez, *Astrophys. J.* **668**, 546 (2007).
- [16] B. D. G. Chandran, T. J. Dennis, E. Quataert, and S. D. Bale, *Astrophys. J.* **743**, 197 (2011).
- [17] B. D. G. Chandran, B. Li, B. N. Rogers, E. Quataert, and K. Germaschewski, *Astrophys. J.* **720**, 503 (2010).
- [18] S. A. Markovskii, B. J. Vasquez, and B. D. G. Chandran, *Astrophys. J.* **709**, 1003 (2010).
- [19] K. T. Osman, W. H. Matthaeus, B. Hnat, and S. C. Chapman, *Phys. Rev. Lett.* **108**, 261103 (2012).
- [20] J. F. Drake and M. Swisdak, *Space Sci. Rev.* **172**, 227 (2012).
- [21] P. A. Isenberg, *Space Sci. Rev.* **95**, 119 (2001).
- [22] P. A. Isenberg and B. J. Vasquez, *Astrophys. J.* **696**, 591 (2009).
- [23] J. He, E. Marsch, C. Tu, S. Yao, and H. Tian, *Astrophys. J.* **731**, 85 (2011).
- [24] C. W. Smith, B. J. Vasquez, and J. V. Hollweg, *Astrophys. J.* **745**, 8 (2012).
- [25] J. C. Kasper, A. J. Lazarus, and S. P. Gary, *Geophys. Res. Lett.* **29**, 20 (2002).
- [26] E. Marsch, in *Reviews in Modern Astronomy*, edited by G. Klare (Springer-Verlag, Berlin, 1991), Vol. 4, p. 138.

- [27] S. P. Gary and K. Nishimura, *J. Geophys. Res.* **109**, 2109 (2004).
- [28] S. P. Gary, C. W. Smith, and R. M. Skoug, *J. Geophys. Res.* **110**, 7108 (2005).
- [29] P. Hellinger, M. Velli, P. Trávníček, S. P. Gary, B. E. Goldstein, and P. C. Liewer, *J. Geophys. Res.* **110**, 12 109 (2005).
- [30] S. P. Gary, L. Yin, D. Winske, J. T. Steinberg, and R. M. Skoug, *New J. Phys.* **8**, 17 (2006).
- [31] J. C. Kasper, A. J. Lazarus, and S. P. Gary, *Phys. Rev. Lett.* **101**, 261103 (2008).
- [32] J. C. Kasper, A. J. Lazarus, J. T. Steinberg, K. W. Ogilvie, and A. Szabo, *J. Geophys. Res.* **111**, 3105 (2006).
- [33] M. Heuer and E. Marsch, *J. Geophys. Res.* **112**, 3102 (2007).
- [34] J. C. Kasper, M. L. Stevens, A. J. Lazarus, J. T. Steinberg, and K. W. Ogilvie, *Astrophys. J.* **660**, 901 (2007).
- [35] A. Verdini and M. Velli, *Astrophys. J.* **662**, 669 (2007).